nature medicine

Angiopoietin-related growth factor antagonizes obesity and insulin resistance

Yuichi Oike[1], Masaki Akao[1], Kunio Yasunaga[2], Toshimasa Yamauchi[3], Tohru Morisada[1], Yasuhiro Ito[1], Takashi Urano[1], Yoshishige Kimura[1], Yoshiaki Kubota[1], Hiromitsu Maekawa[1], Takeshi Miyamoto[1], Keishi Miyata[1], Shun-ichiro Matsumoto[2], Juro Sakai[4], Naomi Nakagata[5], Motohiro Takeya[6], Haruhiko Koseki[7], Yoshihiro Ogawa[8], Takashi Kadowaki[3] & Toshio Suda[1]

Angiopoietin-related growth factor (AGF), a member of the angiopoietin-like protein (Angptl) family, is secreted predominantly from the liver into the systemic circulation. Here, we show that most (>80%) of the AGF-deficient mice die at about embryonic day 13, whereas the surviving AGF-deficient mice develop marked obesity, lipid accumulation in skeletal muscle and liver, and insulin resistance accompanied by reduced energy expenditure relative to controls. In parallel, mice with targeted activation of AGF show leanness and increased insulin sensitivity resulting from increased energy expenditure. They are also protected from high-fat diet–induced obesity, insulin resistance and nonadipose tissue steatosis. Hepatic overexpression of AGF by adenoviral transduction, which leads to an approximately 2.5-fold increase in serum AGF concentrations, results in a significant ($P < 0.01$) body weight loss and increases insulin sensitivity in mice fed a high-fat diet. This study establishes AGF as a new hepatocyte-derived circulating factor that counteracts obesity and related insulin resistance.

Obesity is an increasingly prevalent medical and social problem with potentially devastating consequences because it clusters with type 2 diabetes, hypertension and hyperlipidemia in the metabolic syndrome or syndrome X[1,2]. The molecular mechanisms underlying obesity have not been fully clarified, and effective therapeutic approaches are currently of general interest. Inhibition of weight gain requires that we burn more calories than we take in. From this perspective, adaptive thermogenesis, which is the process of heat production in response to diet or environment temperature, is an important defense against obesity[3,4].

Recently, we and several groups independently identified several molecules containing a coiled-coil domain and a fibrinogen-like domain, motifs structurally conserved in angiopoietins[5,6]. Because these molecules do not bind the angiopoietin receptor, Tie-2, they were named angiopoietin-like proteins (Angptl). We identified angiopoietin-related growth factor (AGF, also known as Angptl6 and encoded by the gene *Angptl6*) as a member of the Angptl family and showed that it is a circulating orphan peptide secreted by liver that induces angiogenesis and proliferation of skin cells, and thereby promotes wound healing[6–8]. Furthermore, several early reports have indicated that there are additional members of the Angptl family, which are currently considered orphan ligands, as angiogenic factors in the vascular system[6,9–11]. On the other hand, several reports indicate that Angptls have biological effects on nonvascular cells. For example, Angptl4 (refs. 12,13; also known as PGAR and FIAF) and Angptl3 (refs. 14,15) regulate fat and/or lipid metabolic homeostasis in addition to controlling angiogenesis[10,11]. These findings suggest that Angptls exert multiple biological functions; however, the physiological and pathological roles of each member of the Angptls have not been fully clarified.

Here we show that most (>80%) of the mice with mutations in AGF (*Angptl6*$^{-/-}$ mice) die at about embryonic day 13, with apparent cardiovascular defects including poorly formed yolk sac and vitelline vessels. Notably, the surviving *Angptl6*$^{-/-}$ mice become markedly obese and have obesity-related metabolic disorders. In parallel, mice with targeted activation of AGF *in vivo* (*Angptl6*-transgenic mice) show markedly reduced adiposity and insulin sensitivity. Furthermore, *Angptl6*-transgenic mice are completely resistant to high-fat diet–induced obesity and impaired insulin sensitivity. Moreover, we found that hepatic overexpression of AGF by adenoviral transduction, which leads to an approximately 2.5-fold increase in serum AGF concentrations, results in a significant ($P < 0.01$) body weight loss and ameliorates insulin sensitivity in mice fed a high-fat diet. Based on these findings, we report here that AGF is a new hepatocyte-derived circulating factor counteracting high-fat diet–induced obesity and related insulin resistance through increased energy expenditure, thereby suggesting a therapeutic potential in counteracting obesity and diabetes.

[1]Department of Cell Differentiation, The Sakaguchi Laboratory, School of Medicine, Keio University, 35 Shinanomachi, Shinjuku-ku, Tokyo 160-8582, Japan. [2]Molecular Medicine Laboratories, Yamanouchi Pharmaceutical Co., Ltd., Tsukuba, 305-8585, Japan. [3]Department of Internal Medicine, Graduate School of Medicine, University of Tokyo, Tokyo 113-8655, Japan. [4]Research Center for Advanced Science and Technology, University of Tokyo, Tokyo 153-8904, Japan. [5]Center for Animal Resources and Development, and [6]Department of Pathology, Kumamoto University, Kumamoto 860-0811, Japan. [7]RIKEN Research Center for Allergy and Immunology, Tsurumi-ku, Yokohama 230-0045, Japan. [8]Department of Molecular Medicine and Metabolism, Medical Research Institute, Tokyo Medical and Dental University, Tokyo 101-0062, Japan. Correspondence should be addressed to Y.O. (oike@sc.itc.keio.ac.jp).

Published online 20 March 2005; doi:10.1038/nm1214

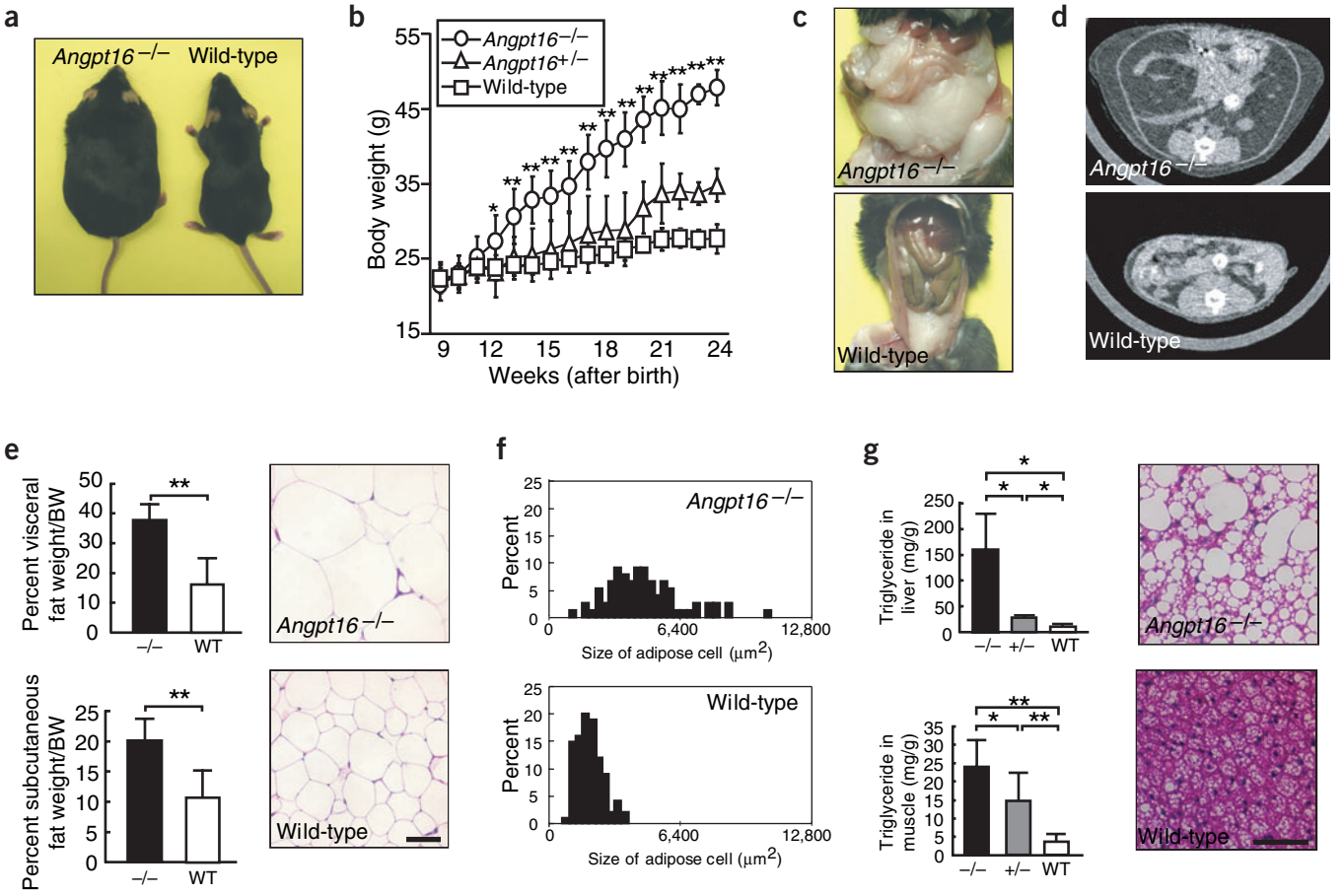

Figure 1 Obesity in *Angptl6*$^{-/-}$ mice on a normal diet. (**a**) Gross appearance of *Angptl6*$^{-/-}$ mice and wild-type control mice. (**b**) Body weight of each genotype ($n = 8$). (**c**–**g**) Abdominal cavity (**c**), CT findings at a level of 8 mm above the top of the iliac bone (**d**), visceral fat ($n = 5$) and subcutaneous fat ($n = 5$) weight/body weight, and histological analysis (**e**) and distribution of cell size (**f**) of WAT of *Angptl6*$^{-/-}$ mice and wild-type mice. (**g**) Triglyceride levels in liver ($n = 5$) and gastrocnemius muscle ($n = 5$), and hematoxylin and eosin–stained sections of BAT of *Angptl6*$^{-/-}$ and wild-type mice. Data are mean ± s.d. Bars in histological sections indicate 50 μm. $^{*}P < 0.05$, $^{**}P < 0.01$, between the two genotypes indicated. Female mice 8 months after birth were used for all experiments.

RESULTS

Disruption of *Angptl6 in vivo*

To investigate the physiological role of AGF, we generated mice with mutations in *Angptl6* (**Supplementary Fig. 1** online). Most (>80%) of *Angptl6*$^{-/-}$ mice die at approximately embryonic day 13 (**Supplementary Fig. 1**), with apparent cardiovascular defects including poorly formed yolk sac and vitelline vessels (data not shown). Notably, the surviving *Angptl6*$^{-/-}$ mice become markedly obese even on a normal chow diet, suggesting that AGF has a crucial role in regulating adiposity in adulthood (**Fig. 1a**). We therefore focused on how AGF functions in the pathogenesis of obesity and associated disorders.

Obesity in *Angptl6*$^{-/-}$ mice

Twelve weeks after birth, *Angptl6*$^{-/-}$ mice showed increases in body weight that surpassed those seen in wild-type (*Angptl6*$^{+/+}$) mice on a normal chow diet (**Fig. 1b**). There were no phenotypic differences between male and female mice. Macroscopic and computed tomographic (CT) analyses taken 8 months after birth showed that both visceral and subcutaneous fat depots were significantly increased in *Angptl6*$^{-/-}$ mice compared to wild-type mice (**Fig. 1c–e**). Sections of white adipose tissue (WAT) from *Angptl6*$^{-/-}$ mice showed increased adipocyte size relative to controls (**Fig. 1e,f**). A large amount of lipid accumulation in liver, skeletal muscle and brown adipose tissue (BAT) was observed in *Angptl6*$^{-/-}$ mice compared with *Angptl6*$^{+/-}$ and wild-type mice (**Fig. 1g**).

Metabolic disorders in *Angptl6*$^{-/-}$ mice

To address alternative causes of increased body weight in *Angptl6*$^{-/-}$ mice, we compared lipid metabolism, rectal temperature, basal metabolic rate and food intake of *Angptl6*$^{-/-}$ and wild-type mice. Significant increases were observed in serum cholesterol and free fatty acid (FFA) concentrations in *Angptl6*$^{-/-}$ mice, whereas there were no significant differences in serum triglyceride concentration between genotypes (**Fig. 2a**). *Angptl6*$^{-/-}$ mice also showed significant decreases in rectal temperature and whole-body oxygen consumption rates compared with wild-type mice (**Fig. 2b**). A small, statistically insignificant increase was observed in daily food intake in *Angptl6*$^{-/-}$ mice compared with controls (**Fig. 2b**).

Adipose tissue has a substantial influence on systemic glucose homeostasis through secretion of adipocytokines[2,16,17]. *Angptl6*$^{-/-}$ mice showed mild hyperglycemia and severe hyperinsulinemia (**Fig. 2c**). To investigate this point further, we performed intraperitoneal glucose and insulin tolerance tests (IGTT and IITT, respectively). Both hyperglycemia and hyperinsulinemia were detected in *Angptl6*$^{-/-}$ mice throughout the time course of the experiment

(**Fig. 2c**). Moreover, the glucose-lowering effect of insulin was decreased in *Angptl6*$^{-/-}$ mice relative to controls, indicating insulin resistance in *Angptl6*$^{-/-}$ mice (**Fig. 2d**). Recent studies have shown a role for tumor necrosis factor (TNF)-α[18,19] secreted from adipose tissue as a mediator of insulin resistance, and adiponectin[20,21] and leptin[22,23] have a role in insulin sensitivity. The leptin concentration in *Angptl6*$^{-/-}$ mice was significantly higher than that seen in controls, whereas no significant differences were observed in adiponectin and TNF-α concentrations between genotypes (**Fig. 2e**).

Molecular alterations in *Angptl6*$^{-/-}$ mice

The physiological data presented above indicate that inactivation of AGF *in vivo* leads to decreased energy expenditure and obesity. Recent studies indicate that BAT and skeletal muscle function as tissues mediating adaptive thermogenesis, which is an important defense against obesity[24,25]. To determine the molecular basis of these metabolic changes in *Angptl6*$^{-/-}$ mice, we examined the expression of molecules with proposed roles in obesity and associated metabolic action in BAT and skeletal muscle. Quantitative RT-PCR analysis showed significant decreases in expression of PPARα, PPARγ, PGC-1β and UCP1 in BAT (**Fig. 2f**) and PPARδ and UCP3 in skeletal muscle (**Fig. 2g**) in *Angptl6*$^{-/-}$ mice, suggesting that such alterations in gene expression underlie susceptibility to obesity in *Angptl6*$^{-/-}$ mice.

Generation of *Angptl6*-transgenic mice

Observations that AGF ablation causes obesity prompted us to further investigate whether AGF functions in resistance to obesity and associated disorders. To generate mice overexpressing AGF constitutively, we targeted the activation of *Angptl6 in vivo* by driving its expression from the chicken β-actin promoter with the cytomegalovirus immediate-early enhancer (CAG promoter)[26,27] (**Supplementary Fig. 2** online). The CAG promoter has been reported to be strongly active in a variety of tissues. In our mice, the promoter drove high expression of the *Angptl6* transgene in BAT, heart and skeletal muscle relative to expression of the endogenous gene in each tissue (**Supplementary Fig. 2**). AGF concentration in the circulation of *Angptl6* transgenic mice increased approximately twofold compared with basal concentrations in nontransgenic controls (**Fig. 3a**).

Leanness in *Angptl6* transgenic mice

Despite a daily food intake similar to that of controls when individually housed and fed a normal chow diet (transgenic mice, 0.17 ± 0.05

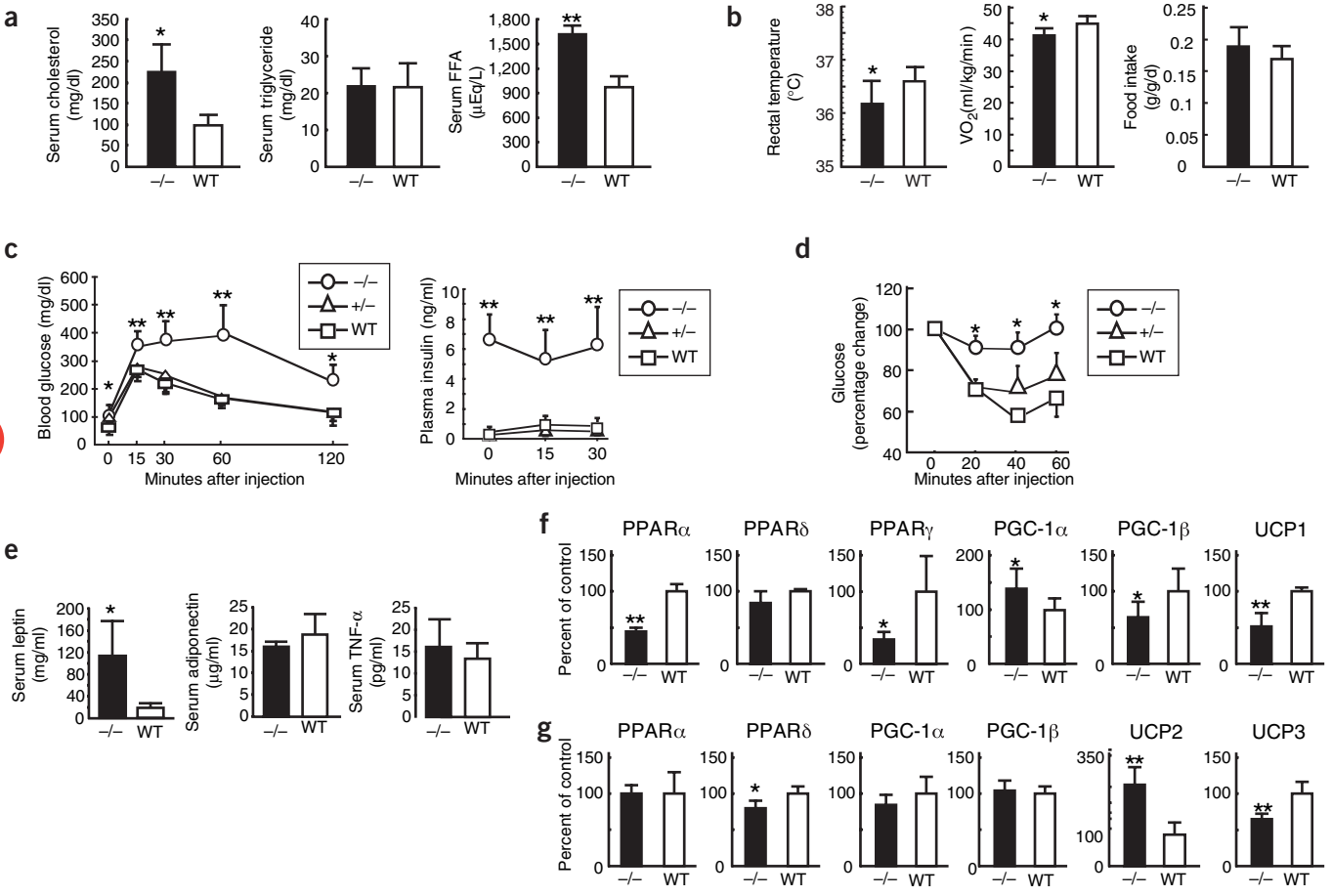

Figure 2 Metabolic effects of AGF deficiency on a normal diet. (**a**) Serum cholesterol, triglyceride and FFA concentrations in *Angptl6*$^{-/-}$ and wild-type control mice at 5 months of age ($n = 5$ in each group). (**b**) Rectal temperature, oxygen consumption (VO_2)/lean body weight and food intake/lean body weight in *Angptl6*$^{-/-}$ and wild-type mice at 6 months of age ($n = 8$ in each group). (**c**,**d**) Glucose (**c**) and insulin (**d**) tolerance tests in *Angptl6*$^{-/-}$, *Angptl6*$^{+/-}$ and wild-type mice at 3 months of age ($n = 6$ in each group). (**e**) Serum leptin, adiponectin, and TNF-α concentrations in *Angptl6*$^{-/-}$ and wild-type mice at 5 months of age ($n = 5$ in each group). (**f**,**g**) Expression of genes associated with energy expenditure in BAT (**f**) and skeletal muscle (**g**) of *Angptl6*$^{-/-}$ relative to wild-type mice (100%) at 3 months of age ($n = 5$ in each group). Data are mean ± s.d. $^*P < 0.05$, $^{**}P < 0.01$, between the two genotypes indicated or among three genotypes. Female mice were used for all experiments.

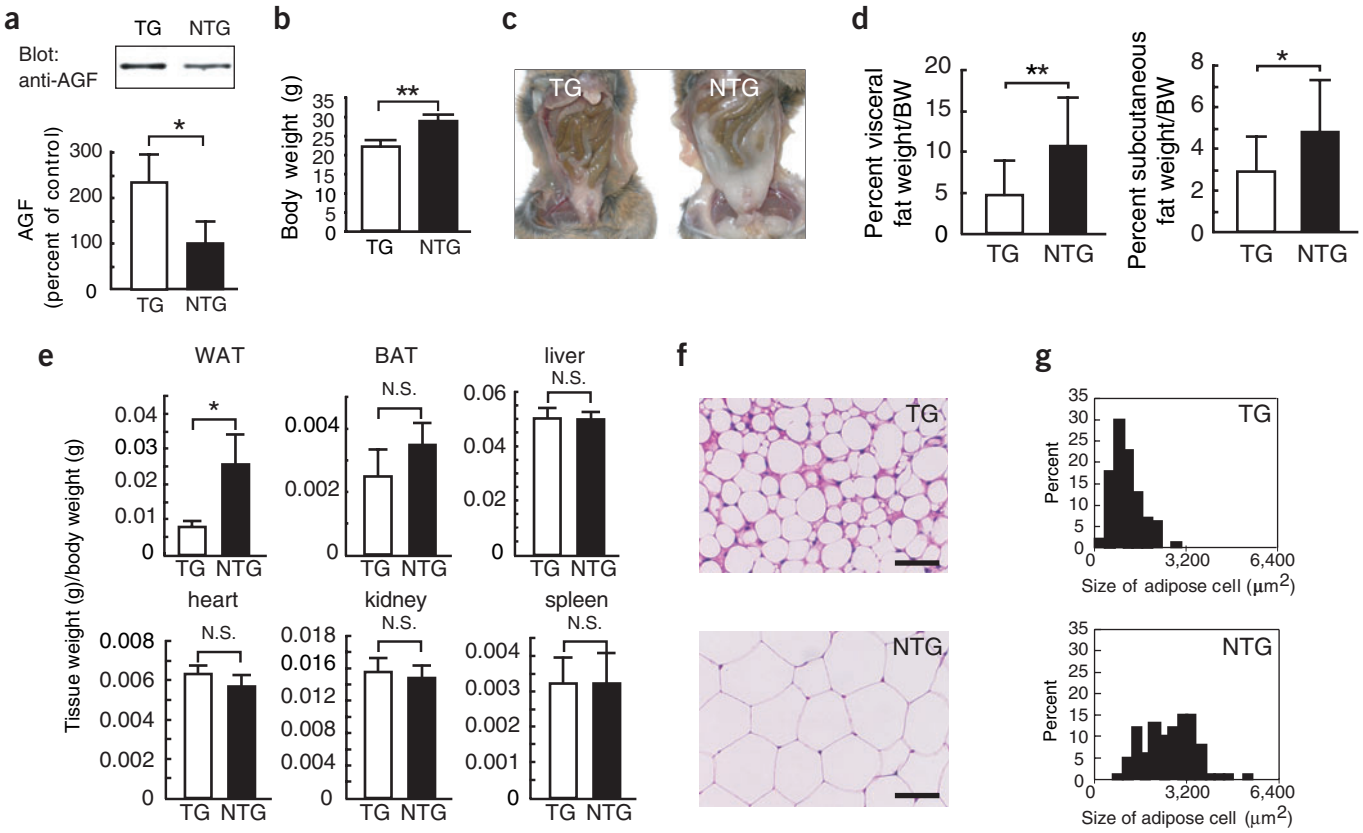

Figure 3 *Angptl6* transgenic mice are lean as a result of a loss of WAT mass. (**a**) Western blotting analysis for serum AGF in *Angptl6* transgenic (TG) and nontransgenic control (NTG) mice at 4 months of age. The ratio for the control is set as 100%. (**b**–**g**) Body weight (**b**), and gross appearance of visceral adipocyte (**c**) in TG and NTG mice at 4 months of age. (**d**) Comparison of visceral fat and subcutaneous fat weight/body weight between TG and NTG mice at 5 months of age. Tissue weight/body weight in TG and NTG mice at 4 months of age (**e**). $n = 10$–15 in each group. Histological analysis (**f**) and distribution of cell size (**g**) of WAT from TG and NTG mice at 4 months of age. Scale bars, 50 μm. Data are mean ± s.d. $^*P < 0.05$, $^{**}P < 0.01$, between the two genotypes indicated. N.S. indicates no significant difference compared with nontransgenic wild-type mice. Female mice were used for all experiments.

versus control mice, 0.15 ± 0.03 g/g lean body mass/d), 5-month-old *Angptl6* transgenic mice showed marked reductions in body weight and adiposity compared with controls (**Fig. 3b–d**). Although there was no alteration in body weight at birth between genotypes, a reduction in body weight of *Angptl6* transgenic mice compared to controls was noted 4 weeks after birth and persisted throughout their life. There were no differences of this alteration in body weight between male and female mice. Furthermore, only WAT weight per body weight in *Angptl6* transgenic mice was markedly decreased compared to that of controls (**Fig. 3e**). Adipocytes from *Angptl6* transgenic mice are smaller in size compared to those from controls, indicating that a reduction in total fat mass may result from decreased triglyceride accumulation (**Fig. 3f,g**).

Metabolic alterations in *Angptl6* transgenic mice

There was no difference in *in vitro* adipocyte differentiation of embryonic fibroblasts between *Angptl6* transgenic mice and controls (data not shown). To address alternative causes for decreased adiposity in *Angptl6* transgenic mice, we compared rectal temperature and basal metabolic rates of *Angptl6* transgenic mice and controls. Transgenic mice showed a small, statistically insignificant increase in rectal temperature and a statistically significant increase in whole-body oxygen consumption rates relative to controls (**Fig. 4a**), suggesting the enhanced energy expenditure in *Angptl6* transgenic mice. The microvasculature assists in heat dissipation at sites of active thermogenesis, increasing the efficiency of lipid release from fat stores[28,29]. *Angptl6* transgenic mice showed an increase in the number of capillary-sized vessels in skeletal muscles compared to controls (**Fig. 4b**), suggesting that AGF assists in part to increase thermogenesis in *Angptl6* transgenic mice.

Quantitative RT-PCR analysis showed significant increases in expression of the genes encoding PPARα, PPARγ and PGC-1β in BAT (**Fig. 4c**) and of the genes encoding PPARα, PPARδ, PGC-1α and UCP2 in skeletal muscle (**Fig. 4d**) in *Angptl6* transgenic mice. These findings suggest that overexpression of AGF *in vivo* activates molecules involved in stimulating energy expenditure, and thereby leads to decreased adiposity.

Insulin sensitivity in *Angptl6* transgenic mice

A lack of fat causes decreases in serum levels of leptin and adiponectin and leads to insulin resistance and diabetes[21,22,30,31]. Although *Angptl6* transgenic mice showed decreased serum leptin levels, identical serum adiponectin levels were observed in transgenic and wild-type mice (**Fig. 4e**). Serum adiponectin levels per WAT mass in *Angptl6* transgenic mice were markedly increased compared with that of wild-type mice, whereas there was no difference in serum leptin levels per WAT mass (**Fig. 4e**), suggesting that adipose tissues in *Angptl6* transgenic mice secrete adiponectin abundantly. Notably, IGTT and IITT showed that *Angptl6* transgenic mice show increased insulin sensitivity despite the greatly decreased serum leptin and identical serum adiponectin levels

(**Fig. 4f**,**g**), suggesting that increased insulin sensitivity observed in *Angptl6* transgenic mice depends on direct effects of increased serum AGF.

Resistance to obesity in *Angptl6*-transgenic mice

To investigate whether *Angptl6* transgenic mice show resistance against developing obesity, we challenged 8-week-old female mice with a high-fat diet containing 32% (wt/wt) fat for 12 weeks to stimulate weight gain. *Angptl6* transgenic mice fed this diet showed significant differences from controls: at the end of the feeding period, the net weight gains were 7.13 ± 1.03 g and 21.86 ± 4.03 g, respectively, for *Angptl6* transgenic and controls (**Fig. 5a**,**b**). As expected, high-fat feeding causes massive lipid accumulation in both visceral and subcutaneous fat depots in controls, whereas few of these changes are seen in *Angptl6* transgenic mice (**Fig. 5c**,**d**). Notably, the size of WAT from *Angptl6* transgenic mice was markedly smaller than that of WAT from controls (**Fig. 5e**). No appreciable fatty acid accumulation in BAT, liver and skeletal muscle was observed in *Angptl6* transgenic mice, whereas nontransgenic mice develop tissue steatosis (**Fig. 5e**,**f**). There was no significant difference in blood glucose levels between genotypes (**Fig. 5g**). But plasma insulin levels in *Angptl6* transgenic mice were much lower than those seen in controls (**Fig. 5g**). Whereas high-fat feeding increases serum cholesterol and FFA levels by twofold in controls, *Angptl6* transgenic mice showed a lipid profile closer to that of wild-type mice fed a standard chow diet (**Fig. 5g**).

AGF antagonizes obesity and insulin resistance

To clarify whether AGF decreases body weight and insulin resistance of obese mice, we intravenously injected adenovirus expressing mouse AGF (Ad-AGF) into female mice fed a high-fat diet containing 32% (wt/wt) fat for 12 months. For controls, adenovirus expressing green fluorescent protein (GFP) (Ad-GFP) was injected. There was no significant difference in body weight between the mice with AGF treatment and controls (54.4 ± 2.2 g and 52.9 ± 2.1 g, respectively: $P = 0.18$, $n = 8$). Throughout the time course of the experiment, mice continued to receive a high-fat diet. On day 20, mice receiving AGF showed approximately 2.5-fold increases in serum AGF levels compared to controls (**Fig. 6a**), and showed significant loss of body weight compared to controls (**Fig. 6b**). No significant difference between the two groups was observed in daily food intake (**Fig. 6c**). Furthermore, significant decreases in fasting and random fed glucose levels were observed in high-fat diet–induced obese mice after treatment with AGF compared to those in controls (**Fig. 6d**,**e**). IGTT and IITT showed that high-fat diet–induced obese mice with AGF treatment showed improved glucose tolerance and increased insulin sensitivity (**Fig. 6f**,**g**). Taken together, these data clearly show that AGF counteracts obesity and related insulin resistance.

DISCUSSION

AGF, a member of the Angptl family, is a circulating angiogenic protein secreted by liver[7]. Here, we show that most (>80%) of the AGF-deficient mice die at approximately embryonic day 13, with apparent cardiovascular defects including poorly formed yolk sac and vitelline vessels. Notably, the surviving *Angptl6*$^{-/-}$ mice become markedly obese and show obesity-related metabolic disorders. Furthermore, *Angptl6*$^{-/-}$ mice show decreased whole-body oxygen consumption and expression of genes involved in energy dissipation. In parallel, *Angptl6* transgenic mice show resistance against diet-induced obesity, insulin resistance and hyperlipidemia. These phenotypes are associated with increases in energy expenditure, supporting the hypothesis that AGF regulates energy metabolism in mice.

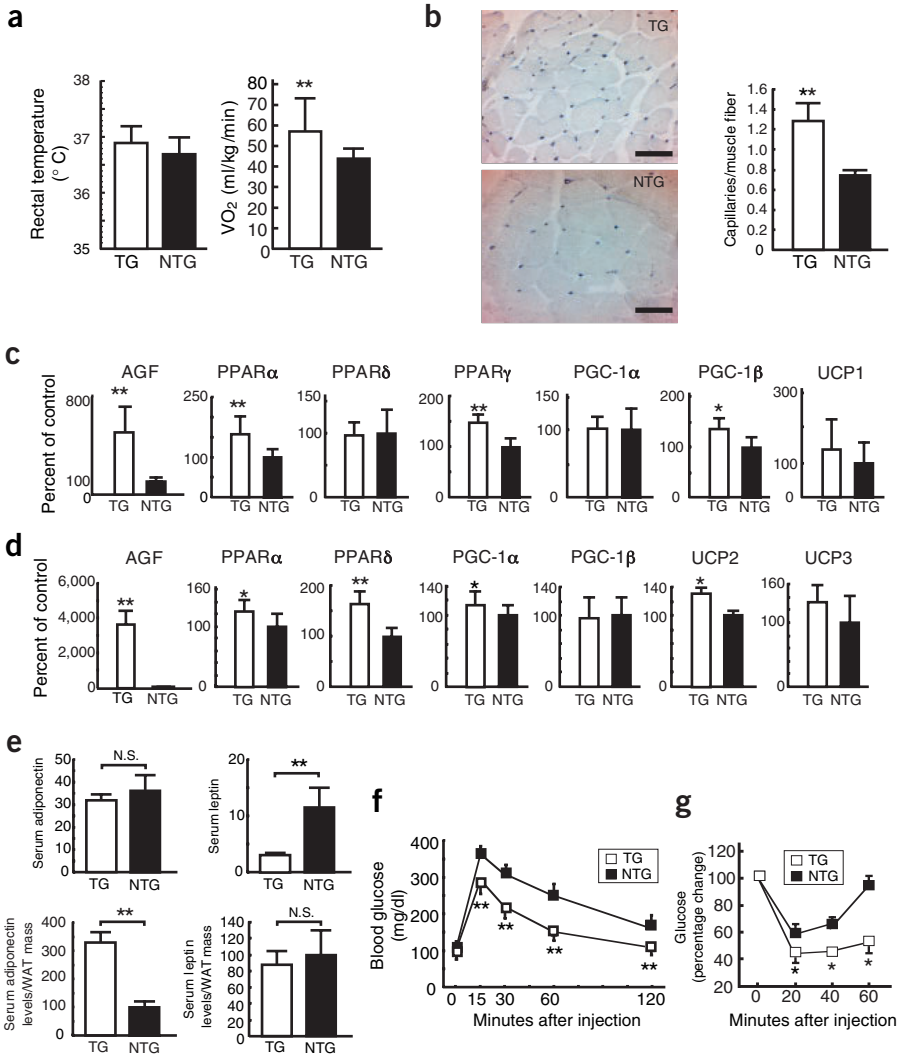

Figure 4 Metabolic and vascular alteration in *Angptl6* transgenic mice. (**a**) Rectal temperature and oxygen consumption (VO_2)/lean body weight in *Angptl6* transgenic (TG) and nontransgenic (NTG) female mice at 5 months of age (n = 10–12 in each group; these mice were also used in **Fig. 4e**,**f**). (**b**) Representative photograph of CD31/PECAM-1-stained capillary vessels and quantitative estimation of capillary vessel density in the gastrocnemius muscle in TG and NTG female mice at 4 months of age. Scale bars, 50 μm. (**c**,**d**) Relative ratio of gene expression associated with increased energy expenditure in BAT (**c**) and skeletal muscle (**d**) in TG mice relative to that seen in NTG female and male mice at 4 months of age. The ratio for the data from NTG mice is set as 100%. (**e**) Serum adiponectin and leptin levels and serum adiponectin and leptin levels/ WAT mass in TG and NTG female mice at 4 months of age. (**f**,**g**) Glucose (**f**) and insulin (**g**) tolerance tests in TG and NTG female mice at 4 months of age. Data are mean ± s.d. (n = 5–15). *P < 0.05, **P < 0.01, between the two genotypes indicated. N.S. indicates no significant difference compared with NTG mice.

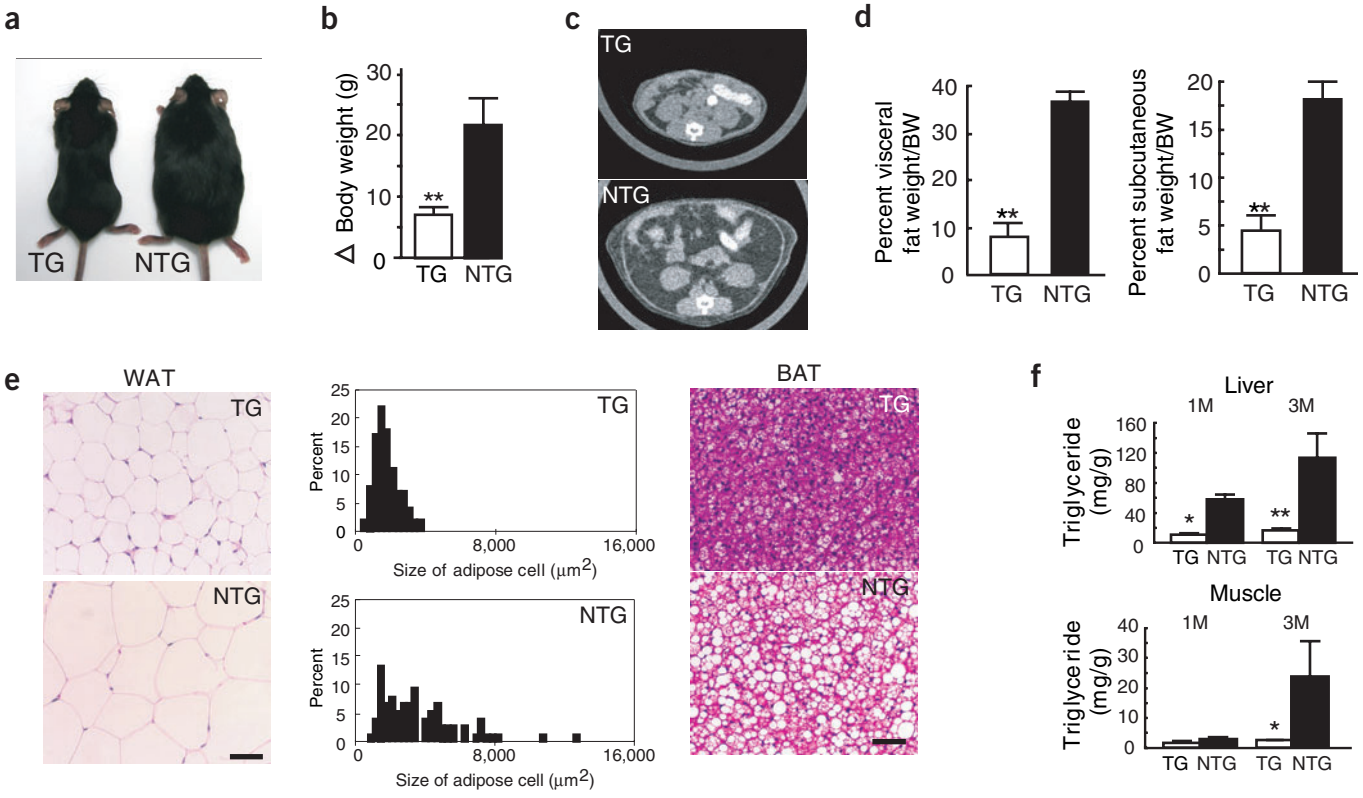

Figure 5 Resistance to high-fat diet-induced obesity and related metabolic disorders seen in *Angptl6* transgenic mice. (**a**) Representative gross appearance of AGF-transgenic (TG) and nontransgenic control (NTG) female mice after 3-months high-fat feeding. (**b**) Change in body weight in TG and NTG male and female mice after 3-months high-fat feeding ($n = 10$). (**c**) CT findings, which were shown at a level of 8 mm above the top of the iliac bone in **a**. (**d**) Visceral fat ($n = 10$) and subcutaneous fat ($n = 10$) weight/body weight. (**e**) Hematoxylin and eosin–stained sections and distribution of cell size of WAT, and hematoxylin and eosin–stained sections of BAT from TG and NTG mice after 3 months of high-fat feeding. (**f**) Triglyceride content in liver ($n = 5$) and gastrocnemius muscle ($n = 5$) from TG and NTG mice after 1 month (left) and 3 months (right) of high-fat feeding. (**g**) Blood glucose, plasma insulin, serum cholesterol, triglyceride, and FFA concentrations in TG and NTG mice after 3-months of high-fat feeding. ($n = 10$ in each group). Scale bars in **e**, 50 μm. Data are mean ± s.d. $^*P < 0.05$, $^{**}P < 0.01$, between the two genotypes indicated.

Metabolic analysis of energy balance using *Angptl6*$^{-/-}$ and *Angptl6* transgenic mice showed that one way AGF functions to regulate adiposity is through control of energy dissipation. Recent studies indicate that BAT and skeletal muscle regulate adaptive thermogenesis, which is mediated by PPARα, PPARδ, PPARγ and their coactivators, PGC-1α and PGC-1β, in response to energy overload[3,16,26,32–35]. We found statistically significant decreases in the expression of PPARα, PPARγ and PGC-1β in BAT and of PPARδ in skeletal muscle in *Angptl6*$^{-/-}$ mice, and increases in expression of PPARα, PPARγ and PGC-1β in BAT and of PPARα, PPARδ, and PGC-1α in skeletal muscle of *Angptl6* transgenic mice. In fact, *Angptl6* transgenic mice show phenotypes similar to those seen in transgenic mice with activated PPARδ[36–38] and PGC-1β[26]. Skeletal muscle is a direct target tissue of AGF, because AGF protein binds to C2C12 myocytes (**Supplementary Fig. 3** online). Treatment of C2C12 myocytes with AGF stimulated ligand activities of PPARα and PPARδ (**Supplementary Fig. 3**). Moreover, AGF activates p38 MAPK in muscle (**Supplementary Fig. 3**), which directly enhances the stabilization and activation of PGC-1 protein[34,35]. We therefore propose that AGF stimulates fat burning in peripheral tissues through the p38 MAPK pathway and downstream effects on respiration and gene expression linked to mitochondrial uncoupling and energy expenditure.

The microvasculature assists in heat dissipation at sites of active thermogenesis in peripheral tissues[28,29]. Because AGF increases the number of capillary-sized vessels in mice[8], we examined whether the vasculature is altered in *Angptl6*$^{-/-}$ and *Angptl6* transgenic mice. *Angptl6*$^{-/-}$ mice were susceptible to obesity and showed significantly ($P < 0.05$) decreased blood-flow perfusion in skeletal muscle, suggesting that loss of AGF enhances observed decreases in the efficiency in energy dissipation (**Supplementary Fig. 4** online). In parallel, a significant ($P < 0.01$) increase in the number of microvessels was observed in skeletal muscle of *Angptl6* transgenic mice, which may antagonize obesity by facilitat-

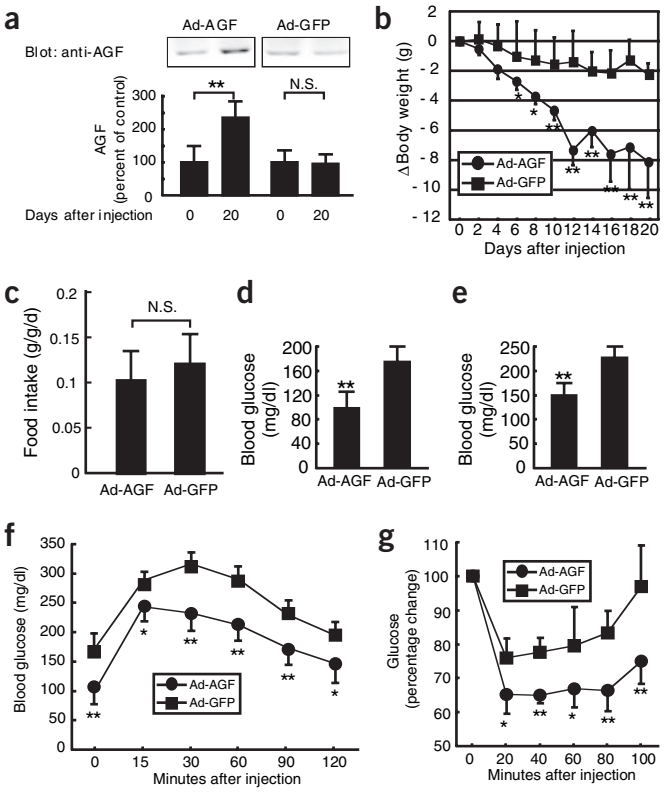

Figure 6 AGF decreased body weight and increased insulin sensitivity in high-fat fed-induced obese mice. (**a**) The relative ratio of serum concentrations of AGF in Ad-AGF injected and Ad-GFP injected mice on day 20 relative to each mouse on day 0. The value of serum AGF concentrations on day 0 is set at 100% ($n = 5$–8 in each group). (**b**) Alteration in body weight of high-fat fed-induced obese female mice after Ad-AGF and Ad-GFP injections ($n = 8$ in each group). (**c**-**g**) Comparison of food intake/lean body weight (**c**), fasting blood glucose (**d**), random fed blood glucose (**e**), glucose tolerance test (**f**) and insulin tolerance test (**g**) between Ad-AGF injected and Ad-GFP injected mice ($n = 5$-8 in each group). Data are mean ± s.d. $^*P < 0.05$, $^{**}P < 0.01$, between the two groups. N.S. indicates no significant difference compared with Ad-GFP–injected mice.

ing increases in energy dissipation. Furthermore, by providing a local angiogenic signal, AGF might increase the efficiency of lipid release from fat stores to maintain energy homeostasis. AGF induces angiogenesis in peripheral tissues, partially explaining how AGF counteracts obesity in addition to the direct effects of AGF on tissues functioning in adaptive thermogenesis.

Recent studies indicate that abnormal accumulation of triglycerides in muscle and liver results in insulin resistance by inhibiting insulin receptor signaling cascades[39,40]. Even on a high-fat diet, *Angptl6* transgenic mice are protected against hepatic and muscle steatosis, resulting in the maintenance of insulin sensitivity. These findings suggest that one mechanism whereby AGF affects insulin sensitivity is inhibition of abnormal lipid stores in insulin target tissues. Adipose tissue has a substantial impact on systemic glucose homeostasis through production of adipokines[34,35]. Recent studies show a role for adiponectin[20,21] and leptin[22,23] as mediators of insulin sensitivity and TNF-α[18,19] in mediating insulin resistance. In lipoatrophic diabetes, adiponectin and leptin deficiency resulting from lack of fat is associated with insulin resistance and diabetes[20,22,30,31]. Despite a greatly decreased WAT mass, *Angptl6* transgenic mice show increased insulin sensitivity, suggesting that AGF may increase insulin sensitivity. In contrast with decreased serum leptin levels, serum adiponectin levels in *Angptl6* transgenic mice were identical to those seen in wild-type mice. This may partially contribute to increased insulin sensitivity in *Angptl6* transgenic mice.

Findings derived from *Angptl6* transgenic mice, in which AGF expression is driven from the CAG promoter, led us to ask whether AGF in the circulation affects obesity and related metabolic abnormalities, because AGF is secreted primarily from hepatocytes. In this study, mice with high-fat diet–induced obesity overexpressing AGF in liver as a result of adenoviral transduction showed 2.5-fold increases in serum AGF levels over in controls and showed significant ($P < 0.01$) body weight loss and improved insulin sensitivity. Moreover, we observed that serum AGF levels in *Angptl6* transgenic mice described here and those seen in K14-*Angptl6* transgenic mice[7,8], in which AGF is driven by a skin-specific (K14) promoter, were approximately identical (**Supplementary Fig. 5** online). Notably, K14-*Angptl6* transgenic mice 8 months after birth show marked reduction in body weight and adiposity compared to controls, and this phenotype is similar to that seen in *Angptl6* transgenic mice created by driving *Angptl6* expression from the CAG promoter (**Supplementary Fig. 5**). K14-*Angptl6* transgenic mice also showed increased insulin sensitivity despite an extremely decreased WAT mass (**Supplementary Fig. 5**). These findings indicate that increasing serum AGF levels could counteract obesity and related insulin resistance, suggesting a physiological role of circulating AGF secreted from liver in antagonizing obesity.

Angptl3 is a circulating factor from liver functioning to regulate lipid metabolism[14,15]. Angptl4 is also predominantly expressed in liver and adipose tissue, and its expression is altered in nutrition and fasting, suggesting a role for Angptl4 in regulating fat metabolism[12,13]. Here, we show that AGF is a new hepatocyte-derived circulating factor counteracting high-fat-induced obesity and related insulin resistance through increased energy expenditure. Taken together with these findings, members of Angptl family function as endocrine factors with overlapping function secreted mainly from the liver to regulate metabolic homeostasis. As a next step to understand the role of Angptl family members in regulating metabolic homeostasis, identification of their cognate receptors and studies aimed at understanding their functional interactions are necessary.

In summary, we provide the first evidence that AGF directly antagonizes obesity and related insulin resistance. In addition to this direct effect, we propose that AGF-induced angiogenesis facilitates increased energy expenditure. Thus, AGF is a potential target for developing attractive pharmacological interventions counteracting obesity and related metabolic diseases.

METHODS

Gene targeting of *Angptl6*, generation of *Angptl6* transgenic mice, cell culture, transcription assays, western blot analyses and laser Doppler blood flow analysis. Please see **Supplementary Methods** online.

Blood analysis and tissue triglyceride assay. For IGTT, female mice were deprived of food 16 h and given 0.75 mg glucose per g body weight intraperitoneally; 3-month-old *Angptl6*$^{-/-}$ mice and controls and 4-month-old *Angptl6* transgenic mice and controls were used ($n = 5$–6 each). For IITT, female mice were given 0.75 U human insulin per kg body weight by subcutaneous injection; 3-month-old *Angptl6*$^{-/-}$ mice and controls and 4-month-old *Angptl6* transgenic mice and controls were used ($n = 5$–6 each). Blood was withdrawn from the supraorbital vein at indicated times. Blood glucose was measured by glucose oxidase method (Sanwa Kagaku). Serum FFA, triglyceride and cholesterol levels were determined by nonesterified fatty acid C-test, triglyceride L-type and cholesterol L-type (Wako), respectively. Plasma insulin was measured by insulin immunoassay (Eiken Kagaku).

Leptin, adiponectin and TNF-α were assayed by leptin assay kit (Linco Research Inc.), ELISA-based adiponectin immunoassay kit (Otsuka Seyaku) and ELISA-based TNF-α immunoassay kit (Techne Corporation), respectively, according to the manufacturer's instructions. Tissues were excised, weighed and homogenized. We added 500 μl of homogenates to 3 ml of methanol/chloroform at 1:2 (vol/vol). The mixture was shaken for 10 min and then centrifuged. We removed the organic layer and saved it, and re-extracted the aqueous layer with 3 ml of methanol/chloroform, and evaporated a small aliquot of the combined organic extracts. The triglyceride concentration of this aliquot was determined as described earlier.

Physiological measurements. For measurement of food consumption, 6-month-old *Angptl6*$^{-/-}$ mice and controls (n = 8 each), and 5-month-old *Angptl6*-transgenic mice and controls (n = 10 each) were housed individually. We measured consumption of food, as well as body weight, for 7 d consecutively. Mice were fed a normal chow diet (CE-2) or a high-fat diet (HFD-32) (CLEA). The high-fat diet study with 6-week-old *Angptl6* transgenic mice and controls was followed for a period of 12 weeks. Rectal temperature was monitored (6-month-old *Angptl6*$^{-/-}$ mice and controls (n = 8 each), and 5-month-old *Angptl6*-transgenic mice and nontransgenic control mice (n = 10 each)) using an electronic thermistor (Model BAT-12) equipped with a rectal probe (RET-3, Physitemp). Oxygen consumption (VO_2) was determined in 6-month-old *Angptl6*$^{-/-}$ mice and controls (n = 5 each), and 5-month-old *Angptl6*-transgenic mice and controls (n = 12 each), with an O_2/CO_2 metabolic measuring system (Model MK-5000, Muromachikikai) at 24 °C as described elsewhere[41]. Mice were kept unrestrained in the chamber for 24 h without food. We determined VO_2 when the minimum plateau shape was obtained during the light cycle, which corresponded to the period of sleep or inactivity. VO_2 is expressed as the volume of O_2 consumed per kilogram weight of lean body mass per minute.

Quantitative RT-PCR. Total RNA was isolated from the BAT and musculus gastrocnemius of mice (6-month-old *Angptl6*$^{-/-}$ mice and controls (n = 5 each), and 6-month-old *Angptl6*-transgenic mice and controls (n = 5 each)). Preparation of DNase-treated total RNA, reverse transcription, and PCR protocols were performed as previously described[8]. The oligonucleotides used for PCR are listed in **Supplementary Table 1** online. We monitored the levels of PCR products with an ABI PRISM 7700 sequence detection system and analyzed them with ABI PRISM 7700 SDS software (Applied Biosystems JAPAN Ltd). The relative abundance of transcripts was normalized to constitutive expression of 18sRNA, β-actin or HPRT mRNA.

CT scan analysis. The adiposity of mice was examined radiographically using CT (LaTheta, ALOKA) according to the manufacturer's protocol. We performed CT scanning at 2-mm intervals from the diaphragm to the bottom of the abdominal cavity.

Hepatic overexpression of AGF by adenoviral transduction. To prepare high-fat diet–induced obese mice, 8-week-old C57BL/6 female mice were fed a high-fat diet containing 32% (wt/wt) fat (HFD-32) for 12 months. Subsequently, mice with high-fat diet–induced obesity (n = 8) received 5×10^9 plaque-forming units (p.f.u.) of Ad-AGF. Serum AGF level was elevated by a single injection of Ad-AGF. For controls, mice with high-fat diet–induced obesity (n = 8) received 5×10^9 p.f.u. of Ad-GFP at the same time. We monitored body weight and food intake daily after intravenous injection of Ad-AGF and Ad-GFP. On day 16 after injection, random fed blood glucose levels were examined. Subsequently, IITT was performed. On day 20 after injection, we examined levels of serum AGF and fasting blood glucose. Subsequently, IGTT was performed.

Statistical analysis and ethical considerations. Results are expressed as the mean ± s.d. or mean ± s.e.m. Differences between groups were examined for statistical significance using Student t test or analysis of variance (ANOVA) with Fisher's PLSD test. The Ethics Review Committee for Animal Experimentation of Keio University approved the experimental protocol.

Note: Supplementary information is available on the Nature Medicine website.

ACKNOWLEDGMENTS

We thank K. Fukushima for her assistance with the experiments. This work was supported by Grants-in-Aid for Scientific Research on Priority Areas from the Ministry of Education, Science and Culture of Japan, by the Yamanouchi Foundation for Research on Metabolic Disorders and by the Mochida Memorial Foundation for Medical and Pharmaceutical Research.

COMPETING INTERESTS STATEMENT

The authors declare competing financial interests (see the *Nature Medicine* website for details).

Received 4 July 2004; accepted 25 January 2005
Published online at http://www.nature.com/naturemedicine/

1. Spiegelman, B.M. & Flier, J.S. Obesity and the regulation of energy balance. *Cell* **104**, 531–543 (2001).
2. Matsuzawa, Y., Funahashi, T. & Nakamura, T. Molecular mechanism of metabolic syndrome X: Contribution of adipokines adipocyte-derived bioactive substances. *Ann. NY Acad. Sci.* **832**, 146–154 (1999).
3. Lowell, B.B., & Spiegelman, B.M. Towards a molecular understanding of adaptive thermogenesis. *Nature* **404**, 652–660 (2000).
4. Levine, J.A., Eberhardt, N.L., & Jensen, M.D. Role of nonexercise activity thermogenesis in resistance to fat gain in human. *Science* **283**, 212–214 (1999).
5. Gale, N.W., & Yancopoulos, G.D. Growth factors acting via endothelial cell-specific receptor tyrosine kinases: VEGFs, Angiopoietins, and ephrins in vascular development. *Genes Dev.* **13**, 1055–1066 (1999).
6. Oike, Y. *et al.* Angiopoietin-related/like protein (ARPs/Angptls) regulate angiogenesis. *Int. J. Hematol* **80**, 21–28 (2004).
7. Oike, Y. *et al.* Angiopoietin-related growth factor (AGF) promotes epidermal proliferation, remodeling and regeneration. *Proc. Natl. Acad. Sci. USA.* **100**, 9494–9499 (2003).
8. Oike, Y. *et al.* Angiopoietin-related growth factor (AGF) promotes angiogenesis. *Blood* **103**, 3760–3766 (2004).
9. Kim, I. *et al.* Molecular cloning, expression, and characterization of angiopoietin-related protein. *J. Biol. Chem.* **274**, 26523–26528 (1999).
10. Camenisch, G. *et al.* ANGPTL3 stimulates endothelial cell adhesion and migration via Integrin αvβ3 and induces blood vessel formation *in vivo*. *J. Biol. Chem.* **277**, 17281–17290 (2002).
11. Ito, Y. *et al.* Inhibition of angiogenesis and vascular leakiness by Angiopoietin-related protein 4. *Cancer Res.* **63**, 6651–6657 (2003).
12. Yoon, J.C. *et al.* Peroxisome proliferator-activated receptor gamma target gene encoding a novel angiopoietin-related protein associated with adipose differentiation. *Mol. Cell Biol.* **20**, 5343–5349 (2000).
13. Kersten, S, *et al.* Characterization of the fasting-induced adipose factor FIAF, a novel peroxisome proliferator-activated receptor target gene. *J. Biol. Chem.* **275**, 28488–28493 (2000).
14. Koishi, R, *et al.* Angptl3 regulates lipid metabolism in mice. *Nat. Genet.* **30**, 151–157 (2002).
15. Inaba, T, *et al.* Angiopoietin-like protein 3 mediates hypertriglyceridemia induced by the liver X receptor. *J. Biol. Chem.* **278**, 21344–21351 (2003).
16. Evans, R.M., Barish, G.D. & Wang, Y.X. PPARs and the complex journey to obesity. *Nat. Med.* **10**, 355–361 (2004).
17. Spiegelman, B.M. & Flier, J.S. Adipogenesis and obesity: Rounding out the big picture. *Cell* **87**, 377–389 (1996).
18. Uysal, K.T., Wiesbrock, S.M., Marino, M.W. & Hotamisligil, G.S. Protection from obesity-induced insulin resistance in mice lacking TNF-α function. *Nature* **389**, 610–614 (1997).
19. Peraldi, P., Xu, M. & Spiegelman, B.M. Thiazolidinediones block tumor necrosis factor-a-induced inhibitor of insulin signaling. *J. Clin. Invest.* **100**, 1863–1869 (1997).
20. Yamauchi, T. *et al.* The fat-derived hormone adiponectin reverses insulin resistance associated with both lipoatrophy and obesity. *Nat. Med.* **7**, 941–946 (2001).
21. Berg, A.H., Combs, T.P., Du, X., Brownlee, M. & Scherer, P.E. The adipocyte-secreted protein Acrp30 enhances hepatic insulin action. *Nat. Med.* **7**, 647–653 (2001).
22. Shimomura, I., Hammer, R.E., Ikemoto, S., Brown, M.S. & Goldstein, J.L. Leptin reverses insulin resistance and diabetes mellitus in mice with congenital lipodystrophy. *Nature* **401**, 73–76 (1999).
23. Friedman, J.M. Obesity in the new millennium. *Nature* **404**, 632–634 (2000).
24. Lowell, B.B., *et al.* Development of obesity in transgenic mice after genetic ablation of brown adipose tissue. *Nature* **366**, 740–742 (1993).
25. Zurlo, F., Larson, K., Bogardus, C. & Ravussin, E. Skeletal muscle metabolism is a major determinant of resting energy expenditure. *J. Clin. Invest.* **86**, 1423–1427 (1990).
26. Kamei, Y. *et al.* PPARγ coactivator 1β/ERR ligand 1 is an ERR protein ligand, whose expression induces a high-energy expenditure and antagonizes obesity. *Proc. Natl. Acad. Sci. USA.* **100**, 12378–12383 (2003).
27. Niwa, H., Yamamura, K. & Miyazaki J. Efficient selection for high-expression transfectants with a novel eukaryotic vector. *Gene* **108**, 193–200 (1991).
28. Sierra-Honigmann, M.R. et al. Biological action of leptin as an angiogenic factor. *Science* **281**, 1683–1686 (1998).
29. Sarmiento, U., *et al.* Morphologic and molecular changes induced by recombinant human leptin in the white and brown adipose tissues of C57BL/6 mice. *Lab. Invest.* **77**, 243–256 (1997).
30. Shimomura, I. *et al.* Insulin resistance and diabetes mellitus in transgenic mice expressing nuclear SREBP-1c in adipose tissue: model for congenital generalized lipodystrophy. *Genes Dev.* **12**, 3182–3194 (1998).
31. Gavrilova, O. *et al.* Surgical implantation of adipose tissue reverses diabetes in

lipoatrophic mice. *J. Clin. Invest.* **105**, 271–278 (2000).
32. Moller, D.E. & Berger, J.P. Role of PPARs in the regulation of obesity-related insulin sensitivity and inflammation. *Int. J. Obes. Relat. Metab. Disord.* **27**, S17–S21 (2003).
33. Wu, Z., *et al.* Mechanisms controlling mitochondrial biogenesis and respiration through the thermogenic coactivator PGC-1. *Cell* **98**, 115–124 (1999).
34. Puigverger, P. *et al.* Cytokine stimulation of energy expenditure through p38 MAP kinase activation of PPARγ coactivator-1. *Mol. Cell* **8**, 971–982 (2001).
35. Puigserver, P. & Spiegelman, B.M. Peroxisome proliferator-activated receptor-γ coactivator 1α (PGC-1α): Transcriptional coactivator and metabolic regulator. *Endocr. Rev.* **24**, 78–90 (2003).
36. Wang, Y.X. *et al.* Peroxisome-proliferator-activated receptor δ activates fat metabolism to prevent obesity. *Cell* **113**, 159–70 (2003).
37. Tanaka, T. *et al.* Activation of peroxisome proliferator-activated receptor delta induces fatty acid beta-oxidation in skeletal muscle and attenuates metabolic syndrome. *Proc. Natl. Acad. Sci. USA.* **100**, 15924–15929 (2003).
38. Dressel, U. *et al.* The peroxisome proliferatior-activated receptor β/δ agonist, GW501516, regulates the expression of genes involved in lipid catabolism and energy uncoupling in skeletal muscle cells. *Mol. Endocrinol.* **17**, 2477–2493 (2003).
39. Shulman, G.I., *et al.* Cellular mechanisms of insulin resistance. *J. Clin. Invest.* **106**, 171–176 (2000).
40. Petersen, K.F. *et al.* Mitochondrial dysfunction in the elderly: Possible role in insulin resistance. *Science* **300**, 1140–1142 (2003).
41. Barger, P.M., Browning, A.C., Garner, A.N. & Kelly, D.P. p38 mitogen-activated protein kinase activates peroxisome proliferator-activated receptor α: a potential role in the cardiac metabolic stress response. *J. Biol. Chem.* **276**, 44495–44501 (2001).